Antidunes on steep slopes

A. Recking, V. Bacchi, Mohamed Naaim, P. Frey

Antidunes on steep slopes

A. Recking, Researcher, Cemagref, UR Erosion Torrentielle Neige Avalanches, 2 rue de la papeterie, BP76, 38402 Saint Martin d'Hères, France. E-mail: alain.recking@cemagref.fr

V. Bacchi, phD Student, Cemagref, UR Erosion Torrentielle Neige Avalanches, 2 rue de la papeterie, BP76, 38402 Saint Martin d'Hères, France. E-mail: vito.bacchi@cemagref.fr

M. Naaim, Researcher, Cemagref, UR Erosion Torrentielle Neige Avalanches, 2 rue de la papeterie, BP76, 38402 Saint Martin d'Hères, France. E-mail: mohamed.naaim@cemagref.fr

P. Frey, Researcher, Cemagref, UR Erosion Torrentielle Neige Avalanches, 2 rue de la papeterie, BP76, 38402 Saint Martin d'Hères, France. E-mail: philippe.frey@cemagref.fr

ABSTRACT

When increasing the rates of subcritical flow on gentle slopes, the bed successively produces ripples, dunes and flat beds. Antidunes (defined here as all bed undulations for which the surface gravity waves are in phase with the bed profile) appear only in high flow rates and may be found in some extreme natural flow events. Inversely, on steep slopes flume experiment ($S \geq 1\%$ approximately) flows are supercritical and antidunes were observed to appear just after the beginning of sediment motion and to disappear for high flow rates. With new experiments, this study aimed to improve the prediction of antidune geometry on steep slopes. An equation for antidune wavelength was deduced from dimensional analysis and fitted to new experimental data. The equation was successfully evaluated using a data set extended to 167 values with data from the literature, obtained on both steep and gentle slopes. This equation gave results very similar to the usual analytical equation from Kennedy when tested on the results from gentle slope experiments, but proved to be better adapted for antidune wavelength on steep slopes.

INTRODUCTION

Flows over natural sediments generally develop bedforms consisting of ripples, dunes and antidunes [*Engelund and Hansen*, 1967; *Gilbert*, 1914; *Van Rijn*, 1984]. Ripples and dunes are downstream migrating bedforms that are triangular in shape with a gently sloping upstream face and a downstream face the slope of which nearly equal the sediment's angle of repose. Antidunes have an approximate sinusoidal shape that is usually characterized by a wave length L and an amplitude A (Figure 1). They were first called antidunes by Gilbert [1914] because they contrast with dunes in their direction of movement. Kennedy [1960] also observed downstream migrating antidunes and extended this term to all forms for which the surface gravity waves are in phase with the bed profile. This definition (including nonmoving sinusoidal shapes) will be considered here. Occurrence of dunes and antidunes depends on the sediment and flow properties. It is generally admitted that ripples are associated with smooth turbulent subcritical flows and dunes are associated with rough turbulent subcritical flows, whereas antidunes are associated with supercritical flows. A better comprehension of the mechanisms controlling bedforms is very important because they are associated with the complex behaviour of both the flow resistance and bedload transport equations. More particularly, a better prediction of antidune geometry can help to analyse local scouring associated with hydraulic structures [*Comiti and Lenzi,* 2006] and to interpret paleo-floods [*Shaw and Kellerhals,* 1977]. Antidune models also represent one (of several) possible mechanisms which may explain the formation of step-pool morphologies in gravel-bed streams [*Chin*, 1999; *Curran*, 2007; *Lenzi*, 2001; *Weichert, et al.*, 2008; *Whittaker and Jaeggi*, 1982].

Several theoretical developments on flow domains pertaining to antidunes were proposed during the last decades [*Carling and Shvidchenko*, 2002; *Colombini*, 2004; *Colombini and*

Stocchino, 2005; 2008; *Deigaard*, 2008; *Engelund*, 1970; *Hayashi*, 1970; *Hayashi and Onishi*, 1983; *Huang and Chiang*, 2001; *Kennedy*, 1960; *Kubo and Yokokawa*, 2001; *Parker*, 1975; *Raudkivi*, 1966; *Reynolds*, 1965; *Sammarco, et al.*, 2006]. All these developments considered analytical solutions for the equations governing the mean flow velocity and sediment bedload transport rate. However, the observations and equations were essentially based on gentle slope experiments. On gentle slopes with fine sands, the bed successively produces ripples, dunes and the flat beds close to transition when increasing the subcritical flow rates. Antidunes appear only for very high flow rates (in the upper regime as defined by Simons and Richardson [1966]) and may characterise extreme natural events. On steep slopes (S>1% approximately) antidunes were also observed for intense sediment transport [*Foley*, 1975; *Smart and Jaeggi*, 1983] but in these (near) supercritical flows, antidunes (as defined above, i.e., a free surface and upper bed layer in phase) were also observed for relatively low flow conditions both in the field (Figure 2 shows antidunes observed on the Arveyron river in june 2009 whereas the flow discharge was estimated to be half the 2 years RI discharge Q_2) and in the flume [*Bathurst, et al.*, 1982a; *Cao*, 1985; *Comiti and Lenzi*, 2006; *Recking, et al.*, 2008a; *Shaw and Kellerhals*, 1977]. Figure 3 presents the images of antidunes obtained with a uniform gravel measuring 4.9 mm in diameter on a 5% slope as part of the steep slope experiments (143 runs) presented in Recking et al [2008a]. This figure shows that for this experiment, antidunes appear very close to the incipient motion flow condition (characterized here by the ratio between the Shields number θ and its critical value for incipient motion θ_c) and that wavelength increased when bed load increased, resulting in a flatter bed as the Shields number increased until the bed become perfectly flat. The shields number is the dimensionless shear stress defined by:

$$\theta = \frac{\tau}{g(\rho_s - \rho)D} = \frac{\rho g R_b S}{g(\rho_s - \rho)D} = \frac{R_b}{D}\frac{S}{(s-1)} \quad (1)$$

where τ is the bed shear stress, R_b is the bed hydraulic radius, D is the grain diameter, ρ_s is the sediment density, ρ is the water density and $s=\rho_s/\rho$ is the relative density. The free surface and bed deformation are maximum for approximately θ/θ_c = 1.5 (suggesting that on steep slopes, antidunes could arise in many natural floods, at least on the rising and falling limbs of the hydrograph), whereas in Simons and Richardson [1966]'s experiments antidunes were observed for θ/θ_c values in the [20-90] range. In both steep and gentle slope experiments, antidunes were obtained in supercritical flows, but for very different transport rates and flow relative depth. This paper aims to verify wether these changing flow conditions affect the antidune geometry by comparing antidunes produced on gentle and steep slopes. More particularly, we will investigate whether wavelength equations proposed for gentle slope flows remain valid on steep slopes, where the flow depth h is on the order of magnitude of the sediment grain size D.

New flume experiments, data from the literature and a semi-empirical investigation of antidune wavelength will provide the analysis. First, a set of dimensionless parameters are deduced from a dimensional analysis. Second, these parameters are used with new steep slope flume experiments (19 runs) to fit a relation giving the antidune wavelength. Third, the model is tested with data from the literature (148 runs) and is compared to existing models. To finish, the results are discussed.

MODELLING

Dimensional analyses

To identify the relevant scaling parameters, we used the dimensional analysis method, which assumes minimal a priori knowledge of antidune dynamics. For the sake of brevity and

clarity, we restricted the analysis to two-dimensional bedforms (also called long-crested antidunes).

The antidune wavelength L can be expressed as a function of nine variables, as represented symbolically by:

$$L = f_1(A, R_b, U, S, \nu, \rho, \rho_s, g, D) \quad (2)$$

where A is the antidune amplitude, R_b is the bed's hydraulic radius (obtained after side wall correction of the measured hydraulic radius $R=hW/[2h+W]$, where h is the flow depth and W is the flow width), U is the mean flow velocity, S is the energy slope, ν is the water viscosity, ρ is the water density, ρ_s is the sediment density, g is the acceleration of gravity and D is the grain diameter. Using the Buckinghams's pi theorem, ten variables involving three basic dimensions would give seven dimensionless pi terms and Eq. 2 could be reduced to:

$$\frac{L}{D} = f_2(F, \mathrm{Re}, \mathrm{Re}^*, \frac{R_b}{D}, S, s) \quad (3)$$

Where $F=U/(gh)^{0.5}$ is the Froude number, $Re=Uh/\nu$ is the Reynolds number, $Re^*=u^*D/\nu$ is the grain Reynolds number (where $u^*=(gRS)^{0.5}=(\tau/\rho)^{0.5}$ is the shear velocity), R_b/D is the relative depth and $s=\rho_s/\rho$ is the relative sediment density. Since flows on steep slopes are rough ($Re^*>70$) and turbulent ($Re>2000$), Re and Re^* can be neglected (both for flow resistance and bedload transport).

In Figure 3 antidunes appear with sediment transport and wavelength increases as flow conditions increase (characterized by the θ/θ_c ratio), with amplitude remaining almost constant (on the order of magnitude of the grain diameter) until the antidunes completely disappears when $\theta=2.5\theta_c$ approximately. For this reason, we suggest looking for a relation linking the antidune geometry to the Shields ratio θ/θ_c. The relative depth R_b/D, the relative

density *s* and the slope *S* can be rearranged to form the Shields number (Eq. 1). The method used in this study is original in that instead of using a constant critical Shields stress θ_c we propose using a variation of this parameter with slope in reference to Lamb et al [2008] and Recking [2009] (this choice will be considered further in the discussion). The following slope-dependent equation proposed in Recking et al [2008b] is used:

$$\theta_c = 0.15S^{0.275} \quad (4)$$

Finally, considering a natural sediment mixture (ρ_s/ρ constant and equal to 2.65), Eq. 3 can be written:

$$\frac{L}{D} = f_3(\theta, \theta_c, F) \quad (5)$$

Experiments

New experiments were conducted at Cemagref to investigate Eq. 5. The experimental setup was a 6-m-long flume. The flume width was varied between 0.05 and 0.102m. We used three uniform sediments – 2.3 mm, 9 mm and 23 mm in diameter – and we varied the slope from 3 to 12.6%. The flow rate at the inlet was ensured by a constant head reservoir and measured by an electromagnetic flowmeter. Before each experiment (for a given material and a given slope), we systematically measured the bed infiltration rate (part of the flow discharge flowing within the gravel bed), which was deduced from the total inlet flow discharge. The sediment feeding system consisted of a customized conveyor belt device ensuring constant feeding (see Recking et al [2008a] for further detail). For each run, measurements were made only after attaining a dynamic equilibrium condition, i.e. near-equality of the feed and trap sediment transport rates, and a near constant time-averaged bed slope. Train antidunes were usually instable and observed over finite distances (generally not affecting the entire flume length). The wavelength *L* was measured by dividing this distance by the number of

147 antidunes. Antidune height was difficult to measure precisely. The flow velocity and the flow
148 depth were deduced from the flow discharge Q using the following friction equation for rough
149 turbulent flows, based on the analysis of 2282 flume and field flow resistance values
150 [*Recking, et al.*, 2008b]:

$$\frac{U}{\sqrt{gR_bS}} = 6.25 + 5.75\log\left(\frac{R_b}{\alpha_{RL}\alpha_{BR}D}\right) \quad (6)$$

151 where U is the vertically averaged flow velocity and

$$\alpha_{RL} = 4\left(\frac{R_b}{D}\right)^{-0.43} \quad \text{with } 1 \le \alpha_{RL} \le 3.5 \quad (7)$$

$$\alpha_{BR} = 7S^{0.85}\frac{R_b}{D} \quad \text{with } 1 < \alpha_{BR} \le 2.6 \quad (8)$$

152 where α_{RL} is a roughness layer coefficient taking into account deviation from the logarithmic
153 profile on small relative depth flows (with an increasing influence of the roughness layer) and
154 α_{BR} is a bedload roughness coefficient taking into account additional flow resistance caused
155 by bedload. This flow resistance equation was derived for flat beds but proved to be valid for
156 flows with nonbreaking wave antidunes. The corresponding wavelength and flow conditions
157 are summarized in Table 1. Φ is the dimensionless solid discharge [*Einstein*, 1950] defined
158 by:

$$\Phi = \frac{q_{sv}}{\sqrt{(s-1)gD^3}} \quad (3)$$

159 Where q_{sv} [m^3/s/m] is the volumetric transport rate per unit width.

160

161 ***Model fitting***

162 A functional relationship between L/D, θ, θ_c and F is sought. The model will be investigated
163 in its simplest form, through a power equation:

$$\frac{L}{D} = \xi \theta^{\alpha} {\theta_c}^{\beta} F^{\gamma} \quad (9)$$

where ξ, α, β and γ are constant values to be fitted from our experimental results. The best fit of Eq. 9 (R^2=0.99) gave the following equation (Figure 4):

$$\frac{L}{D} = 0.093 \frac{\theta}{\theta_c^3} F \quad (10)$$

These coefficients allowed us to minimize to zero the mean error $\bar{\varepsilon}$ (where ε is the difference between the measured and calculated values of L) with a standard deviation $\sigma_\varepsilon = 0.02$.

When rearranged with Eq. 1 and Eq.4, it was possible to eliminate D from both sides, and considering a natural sediment of relative density s=2.65, this equation could be reduced to:

$$\frac{L}{R_b} = 16 S^{0.17} F \quad (11)$$

Similar equations could have been investigated for the antidune amplitude A, but unfortunately, we did not produce enough data to investigate this parameter.

MODEL VALIDATION AND COMPARISON

In this section, we test the models' ability to reproduce measured wavelengths L with available data from the literature.

The data set

We built a data set composed of 148 values from Kennedy [1960], Simons and Richardson [1966], Shaw and Kellerhals [1977], Cao [1985] and Recking [2006], obtained in flume experiments with near uniform sediments. The data from Recking [2006] were produced in a 10-m-long, 0.1-m-wide flume in the Lyon LMFA laboratory (Laboratoire de Mécanique des Fluides et d'Acoustique) and must be distinguished from the new data produced at Cemagref.

For these runs, the flow velocity was not computed but measured with a marker technique similar to the salt dilution technique (see Recking [2006] for further detail). Only a few field values are available from Kennedy [1960]. However, the slope values were missing and, given the fine grain diameter (approximately 0.3 mm), a 0.001 slope was used for the calculations. Actually the exact slope value is not very important because with a slope exponent equal to 0.17, the model distinguishes between gentle and steep slopes. For all runs, R_b was calculated with the measured flow depths, after correction for side wall effects using the procedure proposed by Johnson [1942] and modified by Vanoni and Brooks [1957]. The data set is presented in Table 1 and indicates that antidunes on steep slopes were obtained in the $1.1 < \theta/\theta_c < 2.5$ range, whereas on gentle slopes antidunes were obtained in the $10 < \theta/\theta_c < 90$ range.

The data set was compared to the commonly admitted domain permitting antidunes. These limits were derived analytically and give the minimum Froude number F_m [*Kennedy*, 1960] and the maximum Froude number F_M [*Parker*, 1975; *Reynolds*, 1965] for the formation of antidunes for a given wave number $k=2\pi/L$ and flow depth h:

$$F_m^2 = \frac{\tanh kh}{kh} \tag{12}$$

$$F_M^2 = \frac{1}{kh \tanh kh} \tag{13}$$

These equations were compared to the data set in Figure 5 and gave a good estimate of the flow domain permitting antidunes, whatever the slope. Note that antidunes can also appear for a Froude number as low as 0.8.

206 ***Model validation***

207 Figure 6 presents a comparison between the measured wavelengths and the wavelengths
208 computed with Eq. 11. The widely used wavelength equation proposed by Kennedy [1960]
209 was also used for the comparison (Figure 7):

$$F^2 = \frac{1}{kh} \tag{14}$$

210 Models' efficincy was tested by calculating a relative root mean square error (RRMSE)
211 defined by:

$$RRMSE = \frac{\sqrt{\bar{\varepsilon}^2 + \sigma_\varepsilon^2}}{\overline{L_{mes}}} \tag{15}$$

212 where ε is the error calculated from the difference between the measured and calculated
213 values of L and σ_ε is the standard deviation of ε. The results are presented in Table 3. The
214 new model improves antidune wavelength prediction on steep slopes, but also on gentle
215 slopes. Figure 8 presents the calculated to measured ratios for each model and for increasing
216 slopes. As in a few cases the calculation error associated with Eq. 14 was very large, it was
217 necessary to remove these outliers in order to calculate average values that were truly
218 representative of the data set. The new model gives results to within ±10% for all slope
219 values. The bad score on the 3% slope corresponds to six data from Shaw and Kellerhals
220 [1977] (antidunes were obtained during a bed erosion experiment with no sediment feeding).
221 The model from Kennedy (Eqs. 14) gave similar results with an overestimation on gentle
222 slopes and a progressive decrease of the prediction ratio with increasing slope.

223

224 Because in field applications the available parameters may not be the flow depth h but the
225 flow discharge Q, Eq. 11 was also tested by replacing measured R_b and F with values
226 calculated from the flow discharge Q, using Eq. 6 (the algorithm presented in Recking [2006]
227 takes into account a flume side wall effect). Wavelength prediction was unchanged for steep

slope experiments (RRMSE =0.25). The results were not as good for gentle slope experiments (Kennedy [1960] and Simons and Richardson [1966]) because they were associated with smooth and transitional flows (Re^*<70) for which Eq. 6 is no longer appropriate.

DISCUSSION

Physical significance

Kennedy's equation (Eq.14) was based on the celerity equation for small-amplitude waves [*Milne-Thomson*, 1960] hypothesizing that flows can deform the boundary to conform to a streamline of a wave in a flow of infinite depth. It considers that for a given Froude number F, only one combination is possible between the flow depth h and the bed deformation L. Doing so, it implicitly considers that processes controlling the flow resistance and bed load transport are unchanged whatever the slope. However recent studies have demonstrated that both the mean flow resistance and bedload transport were strongly affected by changing flow hydraulics with changing slope:

(i) First, all the available flume and field data confirmed an increasing critical Shields stress with increasing slope when plotted together [*Recking*, 2009]. This result was first formulated by Shields himself (Shields [1936], pp. 16-17) and was confirmed by several authors after him [*Aksoy*, 1973; *Armanini and Gregoretti*, 2005; *Bathurst*, 1987; *Bathurst, et al.*, 1982b; *Bettess*, 1984; *Bogardi*, 1970; *Graf and Suszka*, 1987; *Mueller, et al.*, 2005; *Shvidchenko and Pender*, 2000; *Shvidchenko, et al.*, 2001; *Tabata and Ichinose*, 1971; *Tsujimoto*, 1991; *Vollmer and Kleinhans*, 2007]. This variation with slope is not as would be expected when studying the gravitational effects acting on the grain alone and several explanations were given for this. Shields considered it was the result of a change in cross-section when the relative depth decreased, whereas others believed it was the consequence of the drag shear stress calculation in presence of form drag at low relative depth [*Buffington*

253 *and Montgomery*, 1997]. However this finding was also confirmed for flows over fine gravels
254 and without bedforms [*Recking*, 2008] which argues for another explanation. Recent analyses
255 considered that gravitational effects acting on the grains are balanced by near bed flow
256 velocity and turbulence changes with changing slope [*Lamb, et al.*, 2008; *Recking*, 2009].
257 Even though the origin of this variation could appear controversial, the critical Shield stress
258 increase with increasing slope is considered here, with several consequences observed not
259 only on bedload transport, but also on flow resistance, as recalled hereafter.
260 (ii) The resulting critical Shields stress function $\theta_c(S)$ improved bedload prediction quite
261 significantly in Recking et al [2008b] when the calculations were based on the concept of
262 excess shear stress (i.e. as $\Phi=f[\theta-\theta_c(S)]$).
263 (iii) We also found that bedload strongly impacts flow resistance [*Recking, et al.*, 2008a].
264 With the findings reviewed above, this explains why a slope-dependent roughness parameter
265 $k_s(S)$ proved to greatly improve mean flow velocity prediction when used in the logarithmic
266 flow resistance equations for U/u^* (Eqs. 6 and 8).
267 These studies produced slope-dependent $\theta_c(S)$, $\Phi(S)$ and $U/u^*(S)$ functions as a consequence
268 of the deviation from the law of the wall on steep slopes and because of flow resistance and
269 bedload interactions. Thus, by impacting all parameters controlling antidunes when the slope
270 is increased, these effects explain why antidune prediction was improved by incorporating the
271 slope in the wavelength equation, through $\theta_c(S)$. In addition, the good score obtained with Eq.
272 11 for any slope value may result from the fitting of the $\theta_c(S)$ function (Eq.4) on the full
273 range of slopes (from 0.001 to 0.1) in Recking [2008b].
274
275 Because it is not the gravitational effects associated with the changing slope that are
276 responsible for the observed changes in antidune geometry but the changing flow hydraulics

277 associated with changing slope, Eq. 11 can be rewritten as a function of the friction
278 coefficient considering $S = (U/u^*)^{-2}F^2$ (where $U/u^* = (8/f)^{0.5}$ is the Darcy Weisbach coefficient):

$$\frac{L}{R_b} = 16F^{1.35}(U/u^*)^{-0.35} \quad (16)$$

279 This equation provides information on the wavelengths in the F-kh plane for a given value of
280 U/u^* (Figure 9). A complete physically based investigation would consist in deriving new
281 theoretical solutions incorporating these findings, but this was not the purpose of this paper.
282
283 ***Antidune amplitude***
284 In Figure 3 antidunes appear with sediment transport and the bed is flattened when the flow
285 condition increases. Table 4 presents the corresponding flow conditions and associated
286 theoretical wavelengths as predicted with Eq.11. It indicates that when $\theta = 2.5\theta_c$ the
287 wavelength should be 26 cm. The flume length captured by images was approximately 20 cm.
288 This suggests that for such high flow conditions antidunes were still presents, but because of
289 the low amplitude (approximately one grain diameter height) and because the short
290 observation window, they could not be observed. Instead, the bed appears flat.
291
292 Given that antidunes were produced with a very wide range of flume widths (0.05–3.2m),
293 another question concerns the effect of flume geometry on antidune geometry (characterized
294 by an amplitude:wavelength ratio). Given that antidune amplitude data are rare, we also used
295 newly produced data to analyse the flume width effect. Figure 10 presents antidune amplitude
296 as a function of the wavelength. The first observation is that antidune geometries measured in
297 our 0.1-m-wide flume are very coherent with the antidune geometries measured by Cao in a
298 0.6-m-wide flume. These steep slope antidunes fit the following equation fairly well
299 (R^2=0.97):

$$A = 0.033L \quad (17)$$

Antidune geometries measured on gentle slopes in a 2.5-m-wide flume experiment by Simons and Richardson [1966] are also coherent with this result despite a wider scatter. This suggests that the flume width had no or little effect on antidune geometry. These aspects should be evaluated through new experiments in a future investigation.

Field implications

The relevance of this research to field problems deserves discussion. Figure 2 presents antidunes observed on a 3% slope gravel bed river (the Arveyon River in Chamonix, France). Successive trains of antidunes with a wavelength of approximately 3m were regularly produced at the same place and migrated upstream very quickly over a distance of approximately 50 m, before disappearing. However, this observation is rare under field conditions. First, it appears to be rare to find supercritical flow conditions for long time periods and long reaches (e.g. Grant [1997]; it may be more typical to observe longitudinal alternation of supercritical and subcritical flows [*Comiti and Lenzi*, 2006]. Moreover, if on some occasions antidunes can be observed after flooding [*Foley*, 1975], antidunes are usually destroyed on falling water stages [*Carling*, 1999], which renders field observations very rare and comparisons difficult. The model fitted the few values presented by Kennedy [1960] in Figure 6 fairly well.

Another important aspect concerns the effect of grain size distribution given that all the experiments presented in this paper were conducted with uniform or near uniform sediments, whereas natural sediments are usually poorly sorted. Smart and Jaeggi [1983] also obtained flat beds with their uniform sediments at high flow intensities (as was illustrated in Figure 3), but they obtained antidunes with nonuniform bed material in these flows. They did not

provide wavelength values but they described “weak” antidunes. We suspect that such weak antidunes did also exist in our experiments (see discussion above), but could not be observed. We did not succeed in isolating the hydraulic specificities that could explain any differences using Smart [1983]’s data. However, it was demonstrated that in presence of grain sorting, hydraulics alone could not reproduce all phenomena associated with sediment transport [*Dietrich, et al.*, 1989; *Iseya and Ikeda*, 1987; *Recking*, 2006] and additional sediment mixture properties are likely needed to fully understand antidunes in poorly sorted sediments.

CONCLUSION

This study intended to investigate antidune characteristics on steep slopes and to compare the results with available results previously obtained on gentle slopes. Using a data set comprising 167 values (19 newly produced data and 148 data from the literature) it was shown that Kennedy’s theoretical model for the dominant wavelength (Eq. 14) provided a good estimation of measured wavelength, but with decreased efficiency (under prediction) as slope increased.

A wavelength model based on dimensional analysis and new steep slope experiments was proposed. This model proved to reproduce adequately steep slope data from the literature, but also, to improve wavelength prediction on gentle slopes when compared to Kennedy’s models. This model incorporates parameters that are similar to previous ones, i.e. the Froude number and the flow depth, but it also takes into account the changes in flow hydraulics through a slope parameter as was demonstrated in Recking [2009]. The available data did not permit to make any definitive conclusion on antidunes’ amplitude.

348 Additional steep slope data are needed to confirm these results. The grain sorting effects on
349 antidune geometry should also be investigated further because all the available data were
350 obtained with uniform sediments only. Only long-crested antidunes were considered. Three-
351 dimensional antidunes are expected to have shorter wavelengths than those reported in this
352 paper [*Kennedy*, 1963].

353 **ACKNOWLEDGMENTS**

354

355 This study was supported by Cemagref and funding was provided by the ECCO-PNRH
356 program from ANR/INSU N^{o}. ANR-05-ECCO-015, and the PGRN (Pole Grenoblois des
357 Risques Naturels). We are grateful to the TSI laboratory of Saint Etienne (Christophe
358 Ducottet, Nathalie Bochard, Jacques Jay, and Jean-Paul Schon).

359

360 The authors would like to thank Dieter Rickenmann and two other anonymous reviewers who
361 greatly contributed to this paper by providing helpful reviews of an earlier version of this
362 manuscript. Our thanks are extended to Rob Ferguson (Associate Editor) who greatly
363 contributed to this paper by providing additional reviews.

364

REFERENCES

Aksoy, S. (1973), The influence of relative depth on threshoàld of grain motion, paper presented at IAHR, Bangkok, Thailand.

Armanini, A., and C. Gregoretti (2005), Incipient sediment motion at high slopes in uniform flow condition, *Water Resources Research*, *41*, 1-8.

Bathurst, J. C. (1987), Critical conditions for bed material movement in steep, boulder-bed streams, paper presented at Erosion and Sedimentation in the Pacific Rim, AIHS Pub. N°165, Proceedings of the Corvallis Symposium.

Bathurst, J. C., W. H. Graf, and H. H. Cao (1982a), Bedforms and flow resistance in steep gravel-bed channels, paper presented at Euromech 156 : Mechanism of sediment transport, Istanbul.

Bathurst, J. C., W. H. Graf, and H. H. Cao (1982b), Initiation of sediment transport in steep channels with coarse bed material, paper presented at Euromech 156: Mechanics of sediment transport, Istanbul.

Bettess, R. (1984), Initiation of sediment transport in gravel streams, *Proc., Institute of the Civil Engineering*, *77, Part 2, March*, 79-88.

Bogardi, J. (1970), Sediment transportation in alluvial streams (International Post-Graduate Course on Hydrological methods for developping water resources management), N°13, lecture notes, Subject 12, Research Institute for Water Research Development / UNESCO, Budapest, Hungary, 133 pp

Buffington, J. M., and D. R. Montgomery (1997), A systematic analysis of eight decades of incipient motion studies, with special reference to gravel-bedded rivers, *Water Resources Research*, *33*, 1993-2027.

Cao, H. H. (1985), Resistance hydraulique d'un lit à gravier mobile à pente raide; étude expérimentale, PhD thesis thesis, 285 pp, Ecole Polytechnique Federale de Lausane, Lausanne.

391 Carling, P. A. (1999), Subaqueous gravel dunes, *Journal of sedimentary research*, *69*, 534-
392 545.
393 Carling, P. A., and A. B. Shvidchenko (2002), The antidune transition in fine gravel with
394 especial consideration of downstream migrating antidunes. Sedimentology, *Sedimentology*,
395 *49*, 1269-1282.
396 Chin, A. (1999), On the origin of step-pool sequences in mountain streams, *Geophysical*
397 *research letters*, *26*, 231-234.
398 Colombini, M. (2004), Revisiting the linear theory of sand dune formation, *Journal of Fluids*
399 *mechanics*, *502*, 1-16.
400 Colombini, M., and A. Stocchino (2005), Coupling and decoupling bed and flow dynamics:
401 fast and slow sediment waves at high Froude numbers, *Physics of Fluids*, *17*.
402 Colombini, M., and A. Stocchino (2008), Finite-amplitude river dunes, *Journal of Fluids*
403 *mechanics*, *611*, 283-306.
404 Comiti, F., and M. Lenzi (2006), Dimensions of standing waves at steps in moutain rivers,
405 *Water Resources Research*, *42*, 1-13.
406 Curran, J. C. (2007), Step-pool formation models and associated step spacing, *Earth Surface*
407 *Processes and Landforms*, *32*, 1611-1627.
408 Deigaard, R. (2008), Breaking antidunes: cyclic behavior due to hysteresis, *Journal of*
409 *Hydraulic Engineering*, *132*, 620-623.
410 Dietrich, W. E., J. W. Kirchner, H. Ikeda, and F. Iseya (1989), Sediment supply and the
411 development of the coarse surface layer in gravel-bedded rivers, *Nature*, *340*, 215-217.
412 Einstein, H. A. (1950), The bed-load function for sediment transportation in open channel
413 flows, Technical Bulletin N°1026, United States Department of Agriculture - Soil
414 Conservation Service, Washington, 71 pp

Engelund, F. (1970), Instability of erodible beds, *Journal of Fluids mechanics (Digital Archive)*, *42*, 225-244.

Engelund, F., and E. Hansen (1967), A monograph on sediment transport in alluvial streams, T. Forlag, Technical University of Denmark, 62 pp

Foley, M. G. (1975), Scour and fill in an ephemeral stream, D. o. G. a. P. Sciences, Contribution N°2658, California institute of Technology, Pasadena

Gilbert, G. K. (1914), The Transportation of Debris by Running Water, Professional paper N°86, US Geological Survey, Washington Government Printing Office, 263 pp

Graf, W. H., and L. Suszka (1987), Sediment transport in steep channels, *Journal of Hydrosciences and Hydraulic Engineering*, *5*, 11-26.

Grant, G. E. (1997), Critical flow constrains flow hydraulics in mobile-bed streams: A new hypothesis, *Water Resources Research*, *33*, 349-358.

Hayashi, T. (1970), Formation of dunes and antidunes in open channels, *Journal of the Hydraulics Division*, *HY2*, 357-366.

Hayashi, T., and M. Onishi (1983), Dominant wave numbers of ripples, dunes and antidunes on alluvial river beds, paper presented at Second International Symposium on River Sedimentation, Nanjing, China.

Huang, L.-H., and Y.-L. Chiang (2001), The formation of dunes, antidunes and rapidly damping waves in alluvial channels, *Int. J. Numer. Anal. Meth. Geomech.*, *25*, 675-690.

Iseya, F., and H. Ikeda (1987), Pulsations in bedload transport rates induced by a longitudinal sediment sorting: a flume study using sand and gravel mixture, *Geografiska Annaler*, *69A*, 15-27.

Johnson, J. W. (1942), The importance of side-wall friction in bed-load investigations, *Civil Eng.*, *12*, 329-331.

439 Kennedy, J. F. (1960), Stationary waves and antidunes in alluvial channels, 172 pp, PhD
440 Thesis, Califonia Institute of Technology, Pasadena, California.
441 Kennedy, J. F. (1963), The mechanics of dunes and antidunes in erodible-bed channels,
442 *Journal of Fluids mechanics (Digital Archive), 16*, 521-544.
443 Kubo, Y., and M. Yokokawa (2001), Theoretical study on breaking of waves on antidunes,
444 *Spec. Publs. int. ass. sediment, 31*, 65-70.
445 Lamb, M. P., W. E. Dietrich, and J.-G. venditti (2008), Is the critical Shields stress for
446 incipient sediment motion dependent on channel-bed slope?, *J. Geophys. Res., 113*.
447 Lenzi, M. A. (2001), Step-pool evolution in the rio Cordon, northeastern Italy, *Earth Surface*
448 *Processes and Landforms, 26*, 991-1008.
449 Milne-Thomson, J. H. (1960), *Theretical hydrodynamics*, New-York.
450 Mueller, E. R., J. Pitlick, and J. M. Nelson (2005), Variation in the reference Shields stress for
451 bed load transport in gravel-bed streams and rivers, *Water Resources Research, 41*, W04006
452 (04001-04010).
453 Parker, G. (1975), Sediment inertia as cause of river antidunes, *Journal of the Hydraulics*
454 *Division, 101*, 211-221.
455 Raudkivi, A. J. (1966), Bedforms in alluvial channels, *Journal of Fluids mechanics (Digital*
456 *Archive), 26*, 507-514.
457 Recking, A. (2006), An Experimental Study of Grain Sorting Effects on Bedload, 261 pp,
458 PhD Thesis Cemagref www.lyon.cemagref.fr/doc/these/recking/index.shtml, Lyon.
459 Recking, A. (2008), Variation du nombre de Shields critique avec la pente, *La Houille*
460 *Blanche, 5*, 59-63.
461 Recking, A. (2009), Theoretical development on the effects of changing flow hydraulics on
462 incipient bedload motion, *Water Resources Research, 45, W04401*, 16.

463 Recking, A., P. Frey, A. Paquier, P. Belleudy, and J. Y. Champagne (2008a), Bedload
464 transport flume experiments on steep slopes, *Journal of Hydraulic Engineering*, *134*, 1302-
465 1310.
466 Recking, A., P. Frey, A. Paquier, P. Belleudy, and J. Y. Champagne (2008b), Feedback
467 between bed load and flow resistance in gravel and cobble bed rivers, *Water Resources*
468 *Research*, *44*, 21.
469 Reynolds, A. J. (1965), Waves on the erodible bed of an open channel, *Journal of Fluids*
470 *mechanics*, *22*, 113-133.
471 Sammarco, P., C. C., M. Trulsen, and K. Trulsen (2006), Nonlinear resonance of free surface
472 waves in a current over a sinusoidal bottom: a numerical study, *Journal of Fluid mechanics*
473 *(Digital Archive)*, *279*.
474 Shaw, J., and R. Kellerhals (1977), Paleohydraulic interpretation of antidune bedforms with
475 applications to antidunes in gravel, *Journal of Sedimentary Petrology*, *47*, 257-266.
476 Shields, A. (1936), Anwendung der Aehnlichkeitsmechanik und der Turbulenzforschung auf
477 die Geschiebebewegung, Mitteilungen der Preussischen Versuchsanstalt fur Wasserbau und
478 Schiffbau, 36 pp, (English Translation by WP Ott and JC Van Uchelen) USDA Soil
479 Conservation Service Cooperative Laboratory, California Institute of Technology, Pasadena,
480 Ca, Hydrodynamics Laboratory Publication N°167, Berlin, Heft 26, 26.
481 Shvidchenko, A., and G. Pender (2000), Flume study of the effect of relative depth on the
482 incipient motion of coarse uniform sediments, *Water Resources Research*, *36*, 619-628.
483 Shvidchenko, A., G. Pender, and T. B. Hoey (2001), Critical shear stress for incipient motion
484 of sand/gravel streambeds, *Water Resources Research*, *37*, 2273.
485 Simons, D. B., and E. V. Richardson (1966), Resistance to flow in alluvial channels,
486 Geological Survey Professional Paper 462-J, Washington, 96 pp

Smart, G. M., and M. N. R. Jaeggi (1983), *Sediment transport on steep slopes*, 89-191 pp., Mitteilungen n°64, Der Versuchsanstalt fuer Wasserbau, Hydrologie und Glaziologie, Eidg. Techn. Hochschule Zuerich, Zurich.

Tabata, S., and Y. Ichinose (1971), An Experimental Study on Critical Tractive Force of Cobble Gravels, *SHIN-SABO, Vol.23, No.4, Ser. No.79*, 12-20.

Tsujimoto, T. (1991), Bed-load transport in steep channels, *Fluvial Hydraulics of Mountain Regions, Lect; Notes Earth Sci. ser., 37*, 89-102.

Van Rijn, L. C. (1984), Sediment transport, Part III : Bed forms and alluvial roughness, *Journal of Hydraulic Engineering, 110*, 1733-1755.

Vanoni, V. A., and N. H. Brooks (1957), Laboratory studies of the roughness and suspended load of alluvial streams, Report N°E-68, Sedimentation Laboratory, California Institute of Technology, Passadena, California, 120 pp

Vollmer, S., and G. Kleinhans (2007), Predicting incipient motion, including the effect of turbulence pressure fluctuations in the bed, *Water Resources Research, 43*, 1-16.

Weichert, R. B., G. R. Bezzola, and H.-E. Minor (2008), Bed morphology and generation of step-pool channels, *Earth Surface Processes and Landforms, 33*, 1678-1692.

Whittaker, J. G., and M. Jaeggi (1982), Origin of step-pool systems in mountain streams, *Journal of the Hydraulics Division, 108*, 758-773.

FIGURES CAPTION

Figure 1: Schematic presentation of antidunes characterized by a sediment wave migration in the upstream direction and a bed surface in phase with the form of the water surface.

Figure 2 : Antidunes on the Arveyron river, a 3% slope gravel bed river in Chamonix (France). The wavelength was approximately 2m.

Figure 3: Images of antidunes for increasing flow conditions characterized by the ratio θ/θ_c. Each image presents the free surface and the moving grains.

Figure 4: Wavelength model fitting

Figure 5: Comparison between equations and available antidune data

Figure 6: Comparison between computed (with Eq. 11) and measured wavelengths (77% of the values are within the envelop ±20%)

Figure 7: Comparison between computed (with Eq. 14) and measured wavelengths (51% of the values are within the envelope ±20%)

Figure 8: Calculated-to-measured wavelength ratio for each model and different slopes (each point represents a slope range, from left to right: S<0.005 - 0.007 - 0.01 - 0.03 - 0.05 - 0.07 - 0.09 - 0.12). Vertical lines represent the standard deviation.

Figure 9 : Wavelengths in the F-kh plane with consideration of U/u* values

Figure 10: Amplitude versus wavelength

TABLES

Run	*W* (m)	*D* (mm)	*S*	*Q* (l/s)	*U* (m/s)	*h* (cm)	Rb/D	U/u*c	F	Re	Re*	θ	θ /θ$_c$	ϕ	*L* (m)	*A* (m)
1	0.05	2.3	0.0300	0.24	0.40	1.20	4.66	7.12	1.17	4800	129	0.085	1.48	5.28E-03	0.114	
2	0.05	2.3	0.0300	0.28	0.42	1.33	5.14	7.12	1.16	5600	136	0.093	1.63	1.76E-02	0.143	
3	0.05	2.3	0.0500	0.19	0.38	0.97	4.06	5.61	1.23	3700	154	0.120	1.87	6.34E-02	0.100	
4	0.05	2.3	0.0700	0.13	0.31	0.84	3.51	4.16	1.08	2600	171	0.149	2.06	7.75E-02	0.095	
5	0.05	2.3	0.0900	0.10	0.29	0.69	2.91	3.77	1.11	2000	177	0.159	2.05	4.05E-02	0.087	
6	0.10	9	0.0516	1.50	0.61	2.41	2.56	5.65	1.26	14737	993	0.084	1.21	2.70E-03	0.295	0.015
7	0.10	9	0.0516	2.00	0.67	2.91	3.08	5.66	1.26	19593	1093	0.101	1.45	1.34E-02	0.360	0.014
8	0.10	9	0.0516	2.50	0.73	3.38	3.50	5.78	1.26	24512	1177	0.117	1.65	3.05E-02	0.399	0.015
9	0.10	9	0.0516	3.00	0.77	3.82	3.96	5.74	1.26	29448	1252	0.133	1.86	5.24E-02	0.431	0.011
10	0.10	9	0.0853	1.00	0.51	1.94	2.11	4.05	1.16	9820	1146	0.111	1.43	1.59E-02	0.243	0.014
11	0.10	9	0.0853	1.30	0.55	2.31	2.53	3.98	1.16	12756	1250	0.132	1.72	4.28E-02	0.315	0.013
12	0.10	9	0.0853	1.50	0.58	2.54	2.76	4.02	1.16	14709	1311	0.146	1.87	6.59E-02	0.349	0.013
13	0.10	9	0.0853	1.70	0.60	2.76	3.02	3.98	1.16	16662	1367	0.158	2.05	9.25E-02	0.350	0.013
14	0.10	9	0.1260	0.87	0.43	1.98	2.21	2.74	0.98	8538	1406	0.168	1.99	1.01E-01	0.243	0.015
15	0.10	9	0.1260	1.00	0.45	2.17	2.42	2.74	0.98	9813	1475	0.184	2.18	1.46E-01	0.237	
16	0.10	9	0.1260	1.10	0.47	2.27	2.55	2.79	1.01	10780	1510	0.193	2.29	1.77E-01	0.274	
17	0.10	23	0.1260	2.50	0.61	4.00	1.73	2.75	0.98	24528	5111	0.133	1.55	3.22E-02	0.446	0.022
18	0.10	23	0.1260	2.70	0.63	4.21	1.80	2.78	0.98	26489	5245	0.140	1.62	4.22E-02	0.465	0.017
19	0.10	23	0.1260	3.00	0.65	4.51	1.94	2.77	0.98	29396	5433	0.150	1.75	6.04E-02	0.555	0.022

Table 1: Flow conditions associated with antidunes

545

N°	Author	Ref	*W* (m)	*D* (mm)	*S*	*Q* (l/s)	*U* (m/s)	*h* (cm)	*Rb/D*	*U/u**	*F*	Re	Re*	θ	θ/θ_c	ϕ	*L* (m)	*A* (m)
1	Recking		0.10	4.9	0.0300	1.40	0.57	2.46	4.57	7.02	1.16	9388	365	0.083	1.45	9.00E-03	0.230	
2	Recking		0.10	4.9	0.0300	1.60	0.60	2.67	4.93	7.12	1.17	10435	379	0.090	1.57	1.60E-02	0.240	
3	Recking		0.10	4.9	0.0500	0.70	0.47	1.49	2.90	5.63	1.23	5393	376	0.088	1.34	9.00E-03	0.140	
4	Recking		0.10	4.9	0.0500	0.80	0.49	1.63	3.18	5.61	1.22	6031	393	0.096	1.46	1.60E-02	0.170	
5	Recking		0.10	4.9	0.0500	0.90	0.51	1.76	3.42	5.62	1.23	6652	408	0.104	1.58	2.50E-02	0.190	
6	Recking		0.10	4.9	0.0500	1.05	0.53	1.98	3.83	5.52	1.20	7520	432	0.116	1.76	4.00E-02	0.200	
7	Recking		0.10	4.9	0.0500	1.20	0.55	2.18	4.21	5.47	1.19	8354	452	0.127	1.94	5.70E-02	0.230	
8	Recking		0.10	4.9	0.0500	1.30	0.56	2.32	4.47	5.40	1.17	8878	466	0.135	2.06	6.90E-02	0.260	
9	Recking		0.10	4.9	0.0500	1.50	0.60	2.50	4.78	5.60	1.21	10000	483	0.145	2.20	8.90E-02	0.290	
10	Recking		0.10	4.9	0.0700	0.60	0.39	1.54	3.06	3.84	1.00	4588	456	0.130	1.80	3.40E-02	0.150	
11	Recking		0.10	4.9	0.0700	0.70	0.44	1.59	3.15	4.28	1.11	5310	463	0.133	1.85	5.30E-02	0.180	
12	Recking		0.10	4.9	0.0700	0.80	0.46	1.74	3.43	4.28	1.11	5935	484	0.146	2.02	7.40E-02	0.190	
13	Recking		0.10	4.9	0.0700	0.90	0.49	1.84	3.61	4.44	1.15	6582	496	0.153	2.12	9.70E-02	0.210	
14	Recking		0.10	9	0.0700	1.20	0.54	2.22	2.37	4.46	1.16	8308	1089	0.100	1.39	1.40E-02	0.260	
15	Recking		0.10	9	0.0700	1.40	0.56	2.50	2.66	4.37	1.13	9333	1153	0.113	1.56	2.60E-02	0.310	
16	Recking		0.10	9	0.0700	1.60	0.60	2.67	2.82	4.54	1.17	10435	1188	0.120	1.66	3.90E-02	0.360	
17	Recking		0.10	9	0.0700	1.90	0.61	3.11	3.29	4.28	1.10	11707	1284	0.140	1.93	6.30E-02	0.380	
18	Recking		0.10	9	0.0900	1.20	0.53	2.26	2.43	3.81	1.12	8260	1251	0.133	1.72	5.60E-02	0.260	
19	Recking		0.10	9	0.0900	1.60	0.57	2.81	3.01	3.69	1.09	10247	1391	0.164	2.12	1.12E-01	0.330	
20	Recking		0.10	9	0.0900	1.70	0.59	2.91	3.08	3.77	1.10	10751	1414	0.169	2.17	1.28E-01	0.380	
21	Cao	105	0.60	22.2	0.0300	60.00	1.14	8.78	3.80	7.24	1.23	77360	3499	0.069	1.21	3.26E-04	0.900	0.040
22	Cao	106	0.60	22.2	0.0300	71.00	1.13	10.47	4.54	6.56	1.11	87715	3823	0.083	1.44	1.19E-03	1.135	
23	Cao	107	0.60	22.2	0.0300	81.00	1.39	9.71	4.15	8.44	1.42	101984	3657	0.076	1.32	6.38E-03	1.395	
24	Cao	108	0.60	22.2	0.0300	92.00	1.40	10.95	4.68	8.01	1.35	112326	3882	0.085	1.49	1.12E-02	1.265	
25	Cao	127	0.60	22.2	0.0300	100.00	1.25	13.33	5.74	6.45	1.09	115385	4300	0.104	1.83	2.05E-02	1.268	
26	Cao	117	0.60	22.2	0.0500	35.00	1.00	5.85	2.57	5.98	1.32	48813	3721	0.078	1.18	1.34E-03	0.620	
27	Cao	118	0.60	22.2	0.0500	40.00	0.93	7.14	3.17	5.01	1.12	53854	4114	0.096	1.46	6.00E-03	0.740	
28	Cao	123	0.60	22.2	0.0500	45.00	0.97	7.70	3.41	5.03	1.12	59681	4270	0.103	1.57	1.06E-02	0.725	
29	Cao	119	0.60	22.2	0.0500	50.00	1.25	6.70	2.92	7.02	1.54	26300	3765	0.089	1.34	1.48E-02	0.888	
30	Cao	120	0.60	22.2	0.0500	60.00	1.38	7.20	3.16	7.45	1.64	28300	3808	0.096	1.45	2.85E-02	1.040	0.050
31	Cao	121	0.60	22.2	0.0500	80.00	1.73	7.70	3.31	9.11	1.99	35500	3901	0.100	1.53	6.35E-02	1.115	0.045
32	Cao	122	0.60	22.2	0.0500	100.00	2.00	8.30	3.54	10.18	2.22	41600	4085	0.107	1.63	1.03E-01	1.010	0.020
33	Cao	130	0.60	22.2	0.0700	30.00	0.94	5.31	2.36	4.96	1.31	42483	4207	0.100	1.39	2.26E-02	0.677	
34	Cao	131	0.60	22.2	0.0700	40.00	1.16	5.70	2.54	5.90	1.55	61300	4094	0.108	1.49	5.01E-02	0.800	
35	Cao	132	0.60	22.2	0.0700	50.00	1.49	6.70	2.45	7.71	1.84	88800	4292	0.104	1.44	1.07E-01	0.880	
36	Cao	133	0.60	22.2	0.0700	60.00	1.42	8.20	3.09	6.54	1.58	102000	4689	0.131	1.81	1.37E-01	0.897	0.040
37	Cao	134	0.60	22.2	0.0700	70.00	1.42	8.22	3.60	6.06	1.58	91585	5203	0.153	2.12	1.40E-01	0.863	0.030
38	Cao	140	0.60	22.2	0.0900	40.00	0.87	7.70	3.41	3.36	1.00	53053	5756	0.187	2.41	9.69E-02	0.715	

39	Cao	141	0.60	22.2	0.0900	50.00	1.11	7.54	3.33	4.34	1.28	66593	5684	0.182	2.35	1.59E-01	0.830	
40	Cao	221	0.60	44.3	0.0300	150.00	1.53	16.30	3.47	7.19	1.21	161997	9415	0.063	1.10	1.15E-03	2.120	
41	Cao	223	0.60	44.3	0.0300	170.00	1.64	17.29	3.65	7.52	1.26	179754	9667	0.066	1.16	1.56E-03	2.000	
42	Cao	231	0.60	44.3	0.0500	90.00	1.37	10.99	2.39	6.01	1.31	109786	10114	0.073	1.10	1.10E-03	1.760	
43	Cao	232	0.60	44.3	0.0500	110.00	1.49	12.31	2.67	6.18	1.35	129985	10683	0.081	1.23	1.01E-02	1.800	
44	Cao	233	0.60	44.3	0.0500	130.00	1.42	15.31	3.32	5.28	1.15	143449	11929	0.101	1.53	1.79E-02	2.250	0.078
45	Cao	234	0.60	44.3	0.0500	150.00	1.65	15.19	3.27	6.19	1.35	165972	11830	0.099	1.51	3.19E-02	2.100	0.070
46	Cao	238	0.60	44.3	0.0700	70.00	1.07	10.94	2.42	3.95	1.03	85482	12036	0.103	1.42	5.57E-03	1.180	0.050
47	Cao	239	0.60	44.3	0.0700	90.00	1.24	12.15	2.67	4.35	1.13	106772	12653	0.114	1.57	2.42E-02	1.500	0.045
48	Cao	240	0.60	44.3	0.0700	110.00	1.30	14.07	3.11	4.23	1.11	124801	13607	0.132	1.83	4.24E-02	1.800	0.060
49	Cao	245	0.60	44.3	0.0900	70.00	1.04	11.24	2.50	3.33	0.99	84870	13857	0.136	1.76	3.30E-02	1.550	0.050
50	Cao	246	0.60	44.3	0.0900	90.00	1.21	12.39	2.75	3.69	1.10	106166	14522	0.150	1.94	5.61E-02	2.000	0.070
51	Cao	247	0.60	44.3	0.0900	110.00	1.37	13.41	2.96	4.03	1.19	126695	15086	0.162	2.09	8.80E-02	2.100	0.070
52	Cao	322	0.60	11.5	0.0100	110.00	1.22	15.00	11.74	10.60	1.01	122215	1322	0.071	1.68	1.11E-02	0.940	
53	Cao	323	0.60	11.5	0.0100	130.00	1.31	16.56	12.76	10.92	1.03	139591	1381	0.077	1.83	1.89E-02	1.020	
54	Cao	324	0.60	11.5	0.0100	150.00	1.42	17.66	13.38	11.56	1.08	157380	1415	0.081	1.92	2.72E-02	1.200	
55	Kenned (flume)	514	3.20	0.549	0.0272	170.07	1.42	3.75	67.45	14.29	2.34	53136	55	1.114	19.97	1.39E+01	0.808	
56	Kenned (flume)	52	3.20	0.549	0.0056	72.55	0.50	4.51	81.87	10.06	0.76	22687	27	0.276	7.71	2.78E-01	0.177	
57	Kenned (flume)	510	3.20	0.549	0.0081	97.52	0.67	4.57	82.04	11.20	1.00	30519	33	0.404	10.10	8.47E-01	0.259	
58	Kenned (flume)	57	3.20	0.549	0.0109	113.58	0.79	4.48	81.04	11.45	1.20	35508	38	0.534	12.37	1.82E+00	0.305	
59	Kenned (flume)	54	3.20	0.549	0.0125	122.20	0.84	4.57	82.02	11.30	1.25	38183	41	0.625	13.82	2.45E+00	0.405	
60	Kenned (flume)	59	3.20	0.549	0.0140	157.29	1.01	4.85	87.65	12.42	1.47	49189	45	0.740	16.04	3.73E+00	0.488	
61	Kenned (flume)	517	3.20	0.549	0.0154	154.61	1.09	4.45	79.81	13.40	1.64	48287	45	0.748	15.65	3.73E+00	0.509	
62	Kenned (flume)	58	3.20	0.549	0.0187	186.72	1.30	4.48	80.72	14.42	1.96	58314	49	0.914	18.22	7.87E+00	0.655	
63	Kenned (flume)	53	3.20	0.549	0.0055	158.77	0.66	7.47	135.15	10.43	0.78	49620	35	0.447	12.56	6.73E-01	0.305	
64	Kenned (flume)	55	3.20	0.549	0.0110	252.13	1.08	7.28	130.90	12.26	1.28	78824	48	0.871	20.11	4.08E+00	0.610	
65	Kenned (flume)	51	3.20	0.549	0.0067	265.51	0.79	10.55	188.57	9.58	0.77	82933	45	0.769	20.22	1.31E+00	0.381	
66	Kenned (flume)	425	3.20	0.233	0.0032	73.14	0.48	4.79	201.73	12.50	0.70	22900	9	0.392	12.66	4.40E-01	0.183	
67	Kenned (flume)	437	3.20	0.233	0.0038	90.09	0.61	4.60	194.97	14.82	0.91	28197	10	0.447	13.86	1.74E+00	0.259	
68	Kenned (flume)	424	3.20	0.233	0.0048	98.71	0.69	4.48	188.90	15.16	1.04	30864	11	0.550	15.91	1.65E+00	0.277	
69	Kenned (flume)	429	3.20	0.233	0.0073	112.69	0.75	4.69	199.01	13.02	1.10	35195	13	0.881	22.71	6.87E+00	0.363	
70	Kenned (flume)	428	3.20	0.233	0.0066	112.09	0.78	4.51	189.99	14.57	1.17	35062	12	0.763	20.15	5.82E+00	0.539	
71	Kenned (flume)	426	3.20	0.233	0.0095	121.90	0.82	4.66	197.11	12.53	1.21	38094	15	1.139	27.23	1.10E+01	0.482	
72	Kenned (flume)	427	3.20	0.233	0.0160	148.66	1.00	4.63	197.40	11.77	1.49	46459	20	1.909	39.79	4.25E+01	0.695	
73	Kenned (flume)	436	3.20	0.233	0.0045	211.40	0.88	7.53	314.82	15.46	1.02	66088	13	0.861	25.30	8.19E+00	0.457	
74	Kenned (flume)	433	3.20	0.233	0.0065	243.21	1.01	7.56	316.28	14.73	1.17	76032	16	1.251	33.18	1.97E+01	0.600	
75	Kenned (flume)	432	3.20	0.233	0.0094	263.43	1.04	7.89	334.27	12.27	1.18	82292	20	1.900	45.82	4.38E+01	0.664	
76	Kenned (flume)	412	0.85	0.233	0.0034	19.36	0.52	4.42	178.28	13.97	0.78	22766	9	0.371	11.69	2.94E-01	0.183	
77	Kenned (flume)	410	0.85	0.233	0.0042	25.44	0.64	4.69	189.00	15.02	0.94	29902	10	0.483	14.45	1.63E+00	0.274	
78	Kenned (flume)	422	0.85	0.233	0.0068	30.73	0.80	4.51	183.44	14.98	1.21	36162	12	0.754	19.88	8.83E+00	0.454	
79	Kenned (flume)	411	0.85	0.233	0.0082	32.00	0.84	4.51	182.74	14.35	1.26	37674	14	0.913	22.69	1.08E+01	0.442	

80	Kenned (flume)	417	0.85	0.233	0.0034	55.38	0.84	7.71	299.24	17.42	0.97	65107	11	0.613	19.62	6.13E+00	0.509	
81	Kenned (flume)	416	0.85	0.233	0.0071	70.08	1.05	7.83	311.17	14.78	1.20	82372	17	1.336	34.80	3.26E+01	0.671	
82	Kenned (flume)	413	0.85	0.233	0.0025	69.37	0.80	10.21	384.98	17.06	0.80	81541	11	0.584	20.20	3.48E+00	0.430	
83	Kenned (flume)	414	0.85	0.233	0.0032	94.01	1.04	10.61	391.12	19.44	1.02	110569	12	0.756	24.55	1.50E+01	0.646	
84	Kennedy(Field)	1		0.157			0.76	7.01	446.50	28.98		52992					0.381	
85	Kennedy(Field)	2		0.185			0.99	12.19	658.92	28.63		120774					0.640	
86	Kennedy(Field)	3		0.45			0.98	5.49	122.00	42.23		53512					0.457	
87	Kennedy(Field)	4		0.32			0.64	6.10	190.63	26.16		39019					0.335	
88	Kennedy(Field)	5		0.41			1.16	14.33	349.51	30.94		165925					0.792	
89	Kennedy(Field)	6		0.41			1.32	18.90	460.98	30.66		248832					0.975	
90	Kennedy(Field)	7		0.38			1.49	24.38	641.58	30.47		364180					1.219	
91	Kennedy(Field)	8		0.38			1.65	39.62	1042.63	26.47		652179					2.164	
92	Kennedy(Field)	9		0.38			2.00	42.06	1106.84	31.14		841033					3.353	
93	Kennedy(Field)	10		0.46			2.44	91.44	1987.83	25.76		2229673					3.048	
94	Kennedy(Field)	11		0.41			1.98	94.49	2304.63	20.57		1871996					4.572	
95	Kennedy(Field)	12		0.41			2.35	121.92	2973.66	21.49		2861414					4.267	
96	Shaw		0.31	8	0.0250	13.00	0.78	5.50	6.38	6.97	1.06	31326	905	0.10	1.78		0.372	
97	Shaw		0.31	8	0.0250	15.90	0.74	7.01	8.26	5.81	0.90	35719	1023	0.13	2.30		0.390	
98	Shaw		0.31	8	0.0370	5.70	0.61	3.05	3.67	5.91	1.12	15571	831	0.08	1.36		0.284	
99	Shaw		0.31	8	0.0370	12.70	0.85	4.90	5.77	6.56	1.23	31516	1044	0.13	2.14		0.390	
100	Shaw		0.31	8	0.0370	17.00	0.80	7.00	8.24	5.17	0.96	38198	1250	0.19	3.05		0.460	
101	Shaw		0.31	8	0.0370	17.00	0.96	5.80	6.79	6.84	1.27	40380	1131	0.15	2.51		0.457	
102	Shaw		0.31	8	0.0370	24.90	0.83	9.80	11.61	4.52	0.85	49699	1477	0.26	4.30		0.558	
103	Shaw		0.31	8	0.0370	11.30	0.86	4.30	5.07	7.09	1.33	28903	977	0.12	1.88		0.338	
104	Simon et al	T3 47	2.44	0.27	0.0028	617.02	1.32	19.20	654.59	18.94	0.96	252845	19	1.115	37.29	2.55E+01	1.036	0.015
105	Simon et al	T3 48	2.44	0.27	0.0049	614.19	1.40	17.98	630.14	15.48	1.06	252139	24	1.881	53.86	4.84E+01	1.433	0.046
106	Simon et al	T3 39	2.44	0.27	0.0081	614.76	1.50	16.76	597.47	13.25	1.17	251907	31	2.941	73.52	1.53E+02	1.524	0.055
107	Simon et al	T3 41	2.44	0.27	0.0095	436.36	1.30	13.72	494.97	11.65	1.12	178931	30	2.847	68.37	1.35E+02	1.341	0.037
108	Simon et al	T4 26	2.44	0.28	0.0033	439.19	1.18	15.24	513.17	17.30	0.97	180232	19	1.018	32.93	1.82E+01	0.762	0.018
109	Simon et al	T4 32	2.44	0.28	0.0047	616.17	1.43	17.68	594.60	16.32	1.09	252715	25	1.695	49.31	5.31E+01	1.036	0.021
110	Simon et al	T4 27	2.44	0.28	0.0053	438.06	1.37	13.11	445.11	17.02	1.21	179767	23	1.437	40.27	4.14E+01	0.945	0.043
111	Simon et al	T4 31	2.44	0.28	0.0059	604.28	1.45	17.07	580.31	14.95	1.12	247642	27	2.086	56.75	6.45E+01	1.158	0.067
112	Simon et al	T4 35	2.44	0.28	0.0082	604.00	1.50	16.46	566.28	13.28	1.18	247326	32	2.793	70.30	1.37E+02	1.829	0.076
113	Simon et al	T4 37	2.44	0.28	0.0082	236.16	1.06	9.14	318.24	12.52	1.12	96991	24	1.581	39.51	3.86E+01	0.914	0.040
114	Simon et al	T4 38	2.44	0.28	0.0093	432.12	1.45	12.19	421.46	13.97	1.33	177259	29	2.370	57.32	1.28E+02	1.372	0.043
115	Simon et al	T4 36	2.44	0.28	0.0101	605.41	1.43	17.37	600.45	11.08	1.09	248358	36	3.668	86.70	2.11E+02	1.737	0.037
116	Simon et al	T5 39	2.44	0.45	0.0036	584.46	1.44	16.76	343.21	19.50	1.12	240665	33	0.761	23.46	9.33E+00	1.128	0.030
117	Simon et al	T5 28	2.44	0.45	0.0037	316.87	1.07	12.19	257.25	16.51	0.98	130807	29	0.569	17.94	5.40E+00	0.792	0.015
118	Simon et al	T5 31	2.44	0.45	0.0043	420.51	1.29	13.41	281.09	17.66	1.13	173320	33	0.735	21.85	8.05E+00	0.975	0.018
119	Simon et al	T5 41	2.44	0.45	0.0047	612.21	1.54	16.46	339.07	18.36	1.21	253347	38	0.958	28.12	1.07E+01	1.189	0.043
120	Simon et al	T5 35	2.44	0.45	0.0049	158.01	0.85	7.62	164.78	14.24	0.99	65032	27	0.492	14.08	2.94E+00	0.671	0.021

121	Simon et al	T5 34	2.44	0.45	0.0055	238.99	1.14	8.53	183.91	17.06	1.24	97028	30	0.611	17.09	5.48E+00	0.762	0.024
122	Simon et al	T5 33	2.44	0.45	0.0061	283.73	1.40	8.23	176.25	20.32	1.56	115386	31	0.648	17.66	7.79E+00	0.853	0.030
123	Simon et al	T5 38	2.44	0.45	0.0062	605.41	1.64	15.24	317.53	17.59	1.34	249909	42	1.192	32.19	1.52E+01	1.158	0.027
124	Simon et al	T5 37	2.44	0.45	0.0062	534.34	1.69	13.11	271.27	19.61	1.49	221314	39	1.021	27.50	1.20E+01	1.158	0.024
125	Simon et al	T5 32	2.44	0.45	0.0066	423.62	1.53	11.28	240.07	18.29	1.46	172902	37	0.953	25.46	1.05E+01	1.128	0.088
126	Simon et al	T5 44	2.44	0.45	0.0090	306.67	1.46	8.53	184.60	17.05	1.59	124341	39	1.007	24.52	1.87E+01	0.914	0.064
127	Simon et al	T5 42	2.44	0.45	0.0099	380.30	1.63	9.45	204.44	17.24	1.70	154368	42	1.219	29.10	1.75E+01	1.097	0.076
128	Simon et al	T5 43	2.44	0.45	0.0101	606.55	1.88	13.11	280.46	16.81	1.66	246881	50	1.714	40.50	2.81E+01	1.768	0.082
129	Simon et al	T6 02	2.44	0.93	0.0092	624.95	1.58	16.15	167.60	13.32	1.26	256041	110	0.932	22.62	5.20E+00	1.494	0.094
130	Simon et al	T8 02	0.61	0.33	0.0080	131.96	1.45	15.24	383.14	14.56	1.19	221109	18	1.857	46.72	2.41E+01	1.676	0.043
131	Simon et al	T8 03	0.61	0.33	0.0091	152.91	1.62	15.85	393.55	15.05	1.30	256041	19	2.179	52.69	7.22E+01	1.859	0.070
132	Simon et al	T9 13	0.61	0.33	0.0070	152.34	1.71	14.94	347.94	19.26	1.41	255381	29	1.464	38.51	5.90E+01	1.341	0.037
133	Simon et al	T9 15	0.61	0.33	0.0091	182.93	1.93	15.85	374.17	18.38	1.55	306283	35	2.061	50.10	1.06E+02	2.530	0.055
134	Simon et al	T9 14	0.61	0.33	0.0098	171.03	1.84	15.54	378.18	16.80	1.49	286652	36	2.241	53.43	6.41E+01	1.280	0.015
135	Simon et al	T10 63	2.44	0.47	0.0057	438.91	1.37	13.11	266.46	16.37	1.20	178968	39	0.924	25.41	8.88E+00	1.036	0.070
136	Simon et al	T10 64	2.44	0.47	0.0058	442.03	1.45	12.50	252.71	17.64	1.31	181310	39	0.885	24.41	9.14E+00	1.036	0.061
137	Simon et al	T10 65	2.44	0.47	0.0057	441.74	1.41	12.80	260.05	17.06	1.26	180659	39	0.900	24.80	8.60E+00	1.036	0.061
138	Simon et al	T10 66	2.44	0.47	0.0058	439.48	1.32	13.72	277.77	15.32	1.14	181440	40	0.966	26.83	8.51E+00	1.006	0.061
139	Simon et al	T10 80	2.44	0.47	0.0064	432.40	1.50	11.89	239.35	17.85	1.39	177900	40	0.936	24.83	1.17E+01	1.036	0.079
140	Simon et al	T10 81	2.44	0.47	0.0063	604.56	1.48	16.76	339.28	14.91	1.15	247819	47	1.306	34.79	1.02E+01	1.341	0.012
141	Simon et al	T10 67	2.44	0.47	0.0065	590.97	1.50	16.15	327.33	15.14	1.19	241762	46	1.285	34.34	9.79E+00	1.219	0.030
142	Simon et al	T10 79	2.44	0.47	0.0065	603.43	1.47	16.76	341.52	14.53	1.15	246286	48	1.349	35.83	1.31E+01	1.189	0.024
143	Simon et al	T10 84	2.44	0.47	0.0074	434.95	1.42	12.50	256.57	15.18	1.29	177881	44	1.148	29.57	1.17E+01	1.097	0.064
144	Simon et al	T10 69	2.44	0.47	0.0073	440.04	1.37	13.11	269.47	14.39	1.20	178968	45	1.204	30.75	1.38E+01	1.128	0.079
145	Simon et al	T10 98	2.44	0.47	0.0082	447.41	1.37	13.41	274.94	13.44	1.20	184357	48	1.364	34.13	2.99E+01	0.945	0.073
146	Simon et al	T10 68	2.44	0.47	0.0074	592.95	1.51	16.15	327.71	14.28	1.20	243731	50	1.472	37.77	1.51E+01	1.219	0.015
147	Simon et al	T10 99	2.44	0.47	0.0081	602.30	1.62	15.24	309.90	15.06	1.33	247122	50	1.513	38.13	3.66E+01	1.219	0.094
148	Simon et al	T10 97	2.44	0.47	0.0096	340.09	1.24	11.28	232.83	12.21	1.18	139903	48	1.355	32.40	1.15E+01	1.036	0.049

Table 2: Data from the literature

Model	Eq.14	Eq.11
Steep slope data (S≥1%, 72 values)	0.47 (R^2=0.78)	0.24 (R^2=0.95)
Gentle slope data (S<1%, 76 values)	0.35 (R^2=0.89)	0.29 (R^2=0.93)
All data (148 values)	0.40 (R^2=0.85)	0.28 (R^2=0.94)

Table 3: Relative root mean square error for model efficiency comparison

W (m)	D (mm)	S	Q (l/s)	U (m/s)	H (cm)	R_b/D	U/u^*_c	F	θ	θ/θ_c	L (m)	A/L
0.1	4.9	0.05	0.80	0.49	1.63	3.18	5.61	1.22	0.10	1.53	0.16	0.0309
0.1	4.9	0.05	0.90	0.51	1.76	3.42	5.62	1.23	0.11	1.69	0.17	0.0287
0.1	4.9	0.05	1.05	0.53	1.98	3.83	5.52	1.20	0.12	1.85	0.19	0.0256
0.1	4.9	0.05	1.20	0.57	2.11	4.05	5.78	1.25	0.13	1.94	0.20	0.0242
0.1	4.9	0.05	1.30	0.57	2.28	4.38	5.55	1.21	0.14	2.08	0.22	0.0224
0.1	4.9	0.05	1.50	0.60	2.50	4.78	5.60	1.21	0.15	2.29	0.24	0.0205
0.1	4.9	0.05	1.70	0.63	2.70	5.14	5.67	1.22	0.16	2.46	0.26	0.0191
0.1	4.9	0.05	2.00	0.69	2.90	5.47	6.02	1.29	0.17	2.60	0.27	0.0179

Table 4 : Increasing flow conditions for the experiment presented in Figure 3 **and antidune wavelengths calculated with Eq.11. The Steepness A/L was calculated by assuming a constant antidune height equals the grain diameter 4.9mm.**

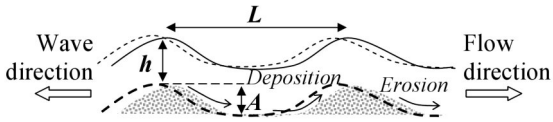

Figure1 : Schematic presentation of antidunes characterized by a sediment wave migration in the upstream direction and a bed surface in phase with the form of the water surface.

Figure 2 : Antidunes on the Arveyron river, a 3% slope gravel bed river in Chamonix (France). The wavelength was approximately 2m.

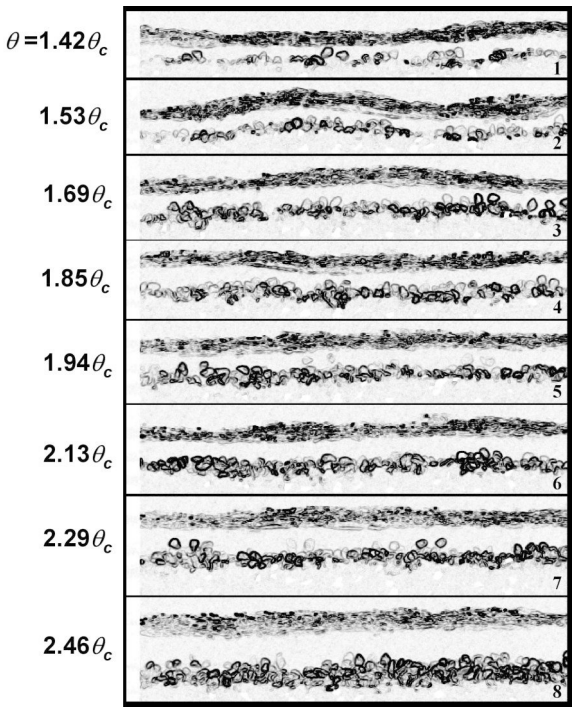

Figure 3 : Images of antidunes for increasing flow conditions characterized by the ratio θ/θ_c. Each image presents the free surface and the moving grains.

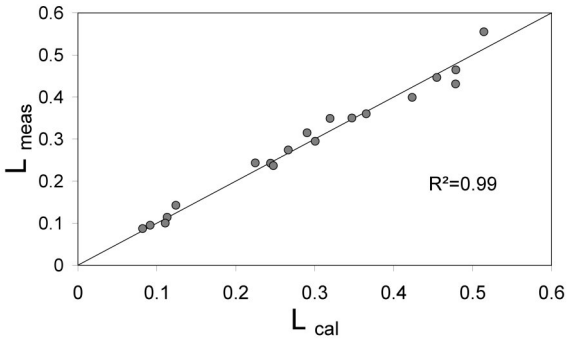

Figure 4: Model fitting

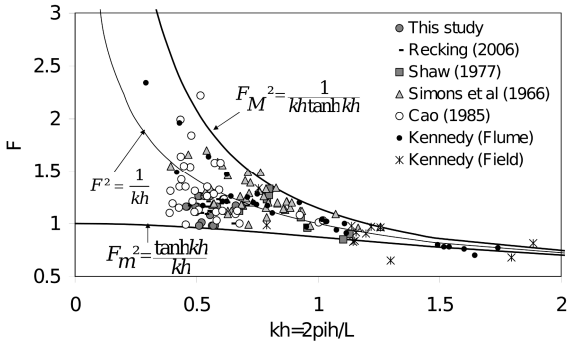

Figure 5 : Comparison between equations and available antidune data

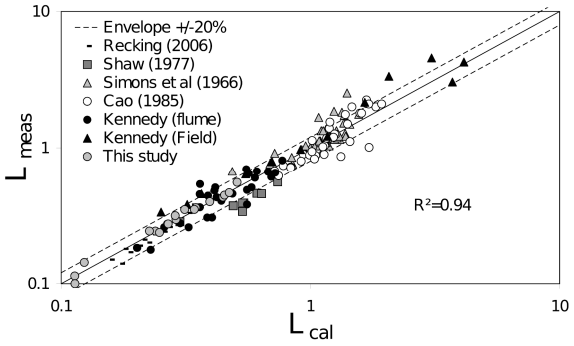

Figure 6: Comparison between computed (with Eq.11) and measured wavelengths (77% of the values are within the envelop ±20%)

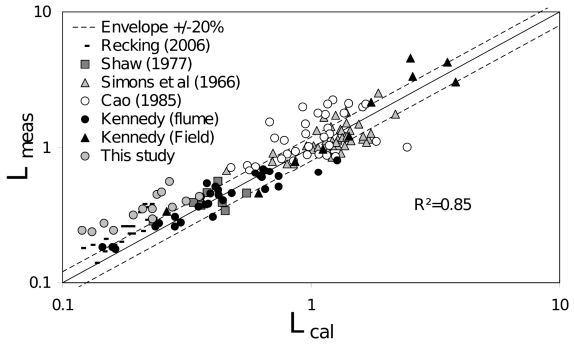

Figure 7: Comparison between computed (with Eq.14) and measured wavelengths (51% of the values are within the envelop ±20%)

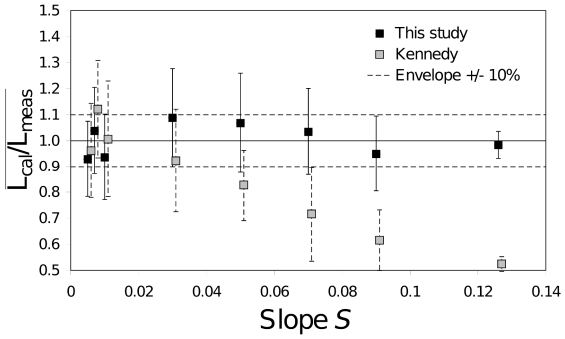

Figure 8: Calculated to measured wavelength ratio for each model and different slopes (each points represent a slope range, from left to right: S<0.005 - 0.007 - 0.01 - 0.03 - 0.05 - 0.07 - 0.09 - 0.12). Vertical lines represent the standard deviation.

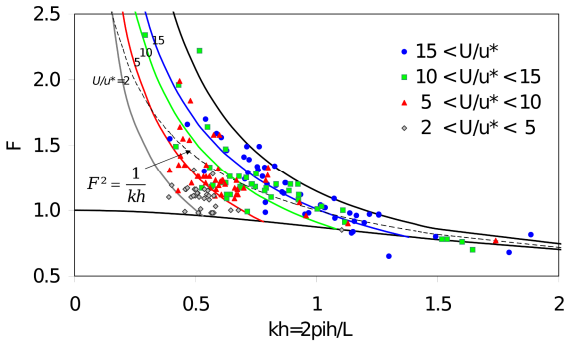

Figure 9 : Wavelengths in the F-kh plane with consideration of U/u* values

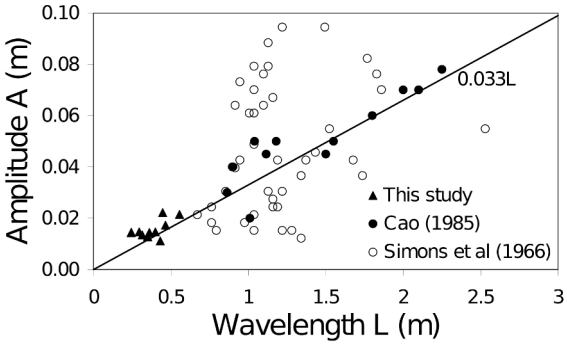

Figure 10: Amplitude versus wavelengths